CHEMISTRY
AN ASIAN JOURNAL

DOI: 10.1002/asia.200900490

Electrografted Poly(*N*-mercaptoethyl acrylamide) and Au Nanoparticles-Based Organic/Inorganic Film: A Platform for the High-Performance Electrochemical Biosensors

Limiao Li,[a, b] Shoujiang Xu,[b] Zhifeng Du,[b] Yanfang Gao,[a] Jinghong Li,*[a] and Taihong Wang*[b]

Abstract: In this study, we describe the use of the combination of eletrografting poly(*N*-mercaptoethyl acrylamide) and Au nanoparticles in the construction of high-performance biosensors. The poly(*N*-mercaptoethyl acrylamide) was electrografted onto the glassy carbon electrode surface, which provided a strongly adhering primer film for the stable attachment of Au nanoparticles and horseradish peroxidase (HRP) enzymes. The performances of the biosensors based on the HRP immobilized in the Au/poly(*N*-mercaptoethyl acrylamide) composite film were investigated. A couple of redox peaks were obtained, indicating that the Au nanoparticles could facilitate the direct-electron transfer between HRP and the underlying electrode. The biosensor showed an excellent electrocatalytic activity toward the reduction of hydrogen oxide and long-term stability, owing to the stable electrografted film and biocompatible Au nanoparticles. Our results demonstrate that the combination of electrografting and Au nanoparticles provides a promising platform for the immobilization of biomolecules and analysis of redox enzymes for their sensing applications.

Keywords: electrochemistry · electrocatalysis · electrografting · horseradish peroxidase · nanoparticles

Introduction

Small molecule detection, such as hydrogen peroxide or glucose, is of importance in wastewater treatment, environmental monitoring, medical sensing, and so on. Much effort has been devoted to develop suitable techniques to precisely monitor concentration with simplicity, high sensitivity, fast response, good selectivity, and low cost. The widely used detection approaches are calorimetry,[1] electrochemiluminescence,[2] electrochemical methods,[3–6] fluorescence spectrometry,[8] and so forth. Among these techniques, various electrochemical methods have attracted considerable interest, owing to their simplicity, short response time, high sensitivity, and excellent selectivity.[3–7] The key issues in developing electrochemical enzymatic biosensors are the effective immobilization of enzymes and reversible direct-electron transfer between the redox centers of enzymes and the electrode surface. Nowadays, the enzyme immobilization strategies generally employed are physical or chemical methods. Physical adsorption is based on the interaction such as van de Waals forces and electrostatic interaction between the enzymes and the transducer. The layer-by-layer (LbL) assembly technique appears as the attractive method, based on alternate adsorption of oppositely charged species on the electrode.[9–11] If the substrate is uncharged, it needs a pretreatment of the surface by dipping in a charged polyelectrolyte solution, which can allow the electrostatic interaction with the first charged layer.[12,13] However, the major problem to be solved is the weak and short-term adhesion between the polyelectrolyte and the substrate. It is often uncontrolled and may not be very stable during the long-term fabrication process. Therefore, covalent bonding at the interface is very important in improving the stability of the pretreatment film.

Electrografting is a method of coating a strongly adhering polymer onto a solid substrate.[14–16] Radical species are

[a] L. Li, Dr. Y. Gao, Prof. J. Li
Key Laboratory of Bioorganic Phosphorus Chemistry & Chemical Biology
Department of Chemistry
Tsinghua University
Beijing, 100084 (China)
Fax: (+86) 10-6277-1149
E-mail: jhli@mail.tsinghua.edu.cn

[b] L. Li, S. Xu, Z. Du, Prof. T. Wang
Micro-Nano Technologies Research Center
Hunan University
Changsha 410082 (China)

 © 2010 Wiley-VCH Verlag GmbH & Co. KGaA, Weinheim

formed following electron transfer from or to the conductive substrate, and finally form covalent bonds with active sites on the electrode. The monomers, in principle, include any cleavable electroactive molecule, including vinylic monomers, acrylic monomers, and diozonium salts.[17–19] Therefore, electrografting can provide a long-term stable film for the subsequent modification of the substrate. Electrografting is an electro-initiated cathodic process, which requires a charged electrode for the grafting step, but not for thickening, as the film is very thin, typically between one monolayer and 50 nm and can be applicable in different kinds of conductor substrates, including metals, carbon, and others. Electrografting has applications in various fields, such as biomolecule immobilization, functionalization, adhesion, template chemistry, and so on.[20–23]

The study of novel nanomaterials has promoted the development of the biomedicine, biosensor, and biocatalyst.[24–28] The biocompatible nanomaterials can provide a moderate microenvironment for enzymes to retain their activity and realize direct electrochemistry. Especially inorganic nanoparticles, owing to their large surface-to-volume ratio, good-electronic conductivity and high-catalytic activity, have been used to immobilize enzymes through the electrostatic interaction between the nanoparticles, and enzymes when constructing biosensors.[29–33] Some noble metals, such as Au nanoparticles (NPs), which have been widely used in the field of biosensors, can act as tiny conduction centers and facilitate electron transfer and simultaneously allow the enzymes to maintain their biocatalytic activities.[34–36] The stability of Au NPs on the electrode surface has a great influence on the performance of biosensors. Thus, it is necessary to explore an efficient method to stably immobilize Au NPs. The widely used method is the attachment of Au NPs on the amine-terminated film through electrostatic interaction.

We have electrografted poly(*N*-mercaptoethyl acrylamide) (PNMEAM) onto a glassy carbon (GC) electrode, which provides thiol bonds for the covalent linking of Au NPs, a strongly adhering primer film for the immobilization of horseradish peroxidase (HRP). The immobilized HRP realized the direct-electron transfer between the active centers and the electrode surface. The HRP/Au/PNMEAM modified electrode showed a fast response and a wide linear range toward reduction of hydrogen oxide and long-term stability, which can be attributed to the stable film and biocompatible Au NPs. The smaller apparent Michaelis–Menten constant, in comparison with the reported values prepared by Au NPs/cystamine modified gold electrode, indicated that the HRP immobilized on the Au/PNMEAM modified electrode retained higher enzymatic activity and affinity for H_2O_2.[37,38]

Abstract in Chinese:

本文中，我们通过结合电接枝 poly(*N*-mercaptoethyl acrylamide)和金纳米颗粒的各自优势来构建了高性能的生物传感器。poly(*N*-mercaptoethyl acrylamide)电接枝在玻碳电极表面，为接下来的金纳米颗粒和 HRP 酶分子的固定提供了稳固的前驱膜。研究了基于固定在 Au/poly(*N*-mercaptoethyl acrylamide) 复合薄膜内的 HRP 酶生物传感器的性能。得到的一对氧化还原峰说明金纳米颗粒可以促进 HRP 与电极间的直接电子转移。生物传感器对双氧水有很好的催化活性并保持了长期的稳定性，这归因于电接枝薄膜的长期稳定性和金纳米颗粒的优良的生物相容性。我们的结果说明电接枝和金纳米颗粒的结合为固定生物分子和研究氧化还原酶的传感性能提供了一个很有前景的平台。

Results and Discussion

Constructing Au/PNMEAM/GC Electrode Surfaces

The ATR-FTIR spectra for the poly(*N*-succinimidyl acrylate) (PNSA)/GC and PNMEAM/GC electrodes can be seen in Figure 1, curves a and b, respectively. Curve a in Figure 1 confirms the expected structure of the PNSA film with characteristic C=O vibrations at $\tilde{\nu}=1744\ cm^{-1}$ and C–N vibration at $\tilde{\nu}=1168\ cm^{-1}$.[16] The spectrum of the SH-terminated surface shows that the typical peaks for PNSA disappear and two peaks, located at $\tilde{\nu}=2532$ and $3375\ cm^{-1}$, corresponding to S–H vibrations and N–H stretching appear, revealing that the ester group was substituted by aminoethanethiol. The SEM image in Figure 2 shows the Au/PNMEAM/GC electrode surface. Au nanoparticles with a diameter of less than 10 nm were uniformly distributed on the PNMEAM-modified electrode surface. To confirm the covalent linking of Au nanoparticles, the electrode was pre-

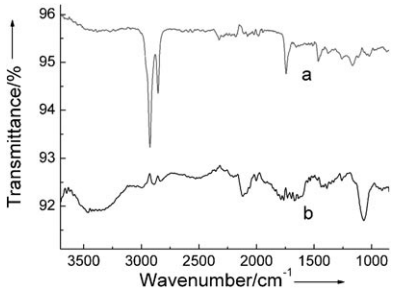

Figure 1. ATR-FTIR spectra for the a) PNSA/GC and b) PNMEAM/GC electrodes.

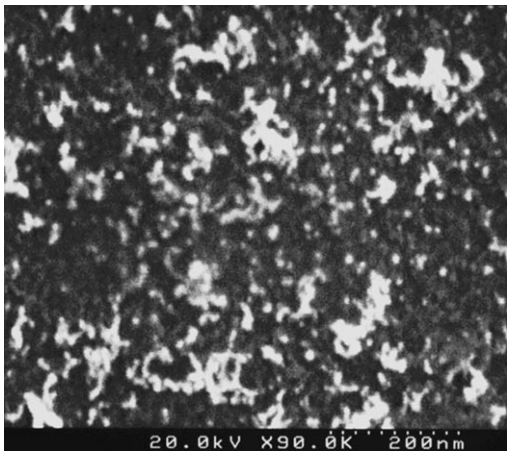

Figure 2. SEM image of Au/PNMEAM/GC electrode surface.

 © 2010 Wiley-VCH Verlag GmbH & Co. KGaA, Weinheim

pared under the same conditions, but without the electrografted film. Almost no Au nanoparticles were observed on the bare glassy carbon electrode surface. As the metal nanoparticles are difficult to stably attach onto the carbon electrode without modification, the advantage of electrografting is that it could provide strongly adhering anchoring sites for the linkage of nanoparticles.

Electrochemical Behaviors of the Modified Electrodes

To study the electrochemical properties of the modified electrodes, the cyclic voltammograms (CVs) and Nyquist plots of impedance measurements were measured (Figure 3) at bare GC (curve a), PNSA/GC (curve b), PNMEAM/GC (curve c), and Au/PNMEAM/GC (curve d) electrodes, respectively. Well-defined CV curves of $[Fe(CN)_6]^{3-/4-}$ on the four electrodes are shown in Figure 3A, indicating quasi-reversible electron-transfer kinetics for the electrode interfaces. However, in comparison with the bare GC electrode, Faradaic current of $[Fe(CN)_6]^{3-/4-}$ at PNSA/GC was attenuated as NSA was electrografted onto the electrode surface and the peak-to-peak separation (ΔE_p) at the PNSA-modified electrode was also increased from 76 mV to 110 mV, indicating that the PNSA film acted as the inert electron and mass transfer blocking layer, and hindered the diffusion of ferricyanide toward the electrode surface. Subsequently the PNMEAM-modified electrode was kept in the aminoethanethiol solution for 12 h, and was tested to show improved reversibility in the electrode reaction (the ΔE_p decreased to 91 mV). If the Au NPs were linked to the electrode, the anodic and cathodic current responses were even better than those of the bare electrode with $\Delta E_p = 73$ mV. According to the Laviron model, the heterogeneous electron transfer rate constant (k_s) was estimated to be 0.0165 $cm\,s^{-1}$, by assuming a one-electron transfer process, which was higher than those of bare electrode (0.0145 $cm\,s^{-1}$), PNSA-modified electrode (3.69×10^{-3} $cm\,s^{-1}$), and PNMEAM-modified electrode (6.44×10^{-3} $cm\,s^{-1}$). This demonstrated that the Au NPs assembled on the glassy carbon electrode surface promoted the electron transfer between the analyte and the electrode surface.

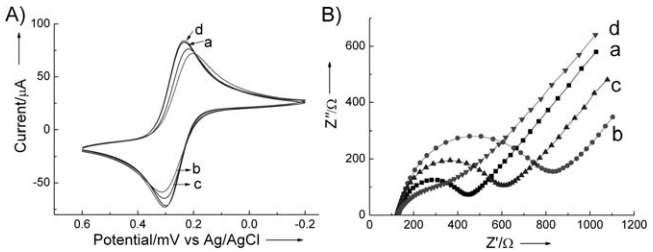

Figure 3. Cyclic voltammograms of 5 mM $[Fe(CN)_6]^{3-/4}$ at a bias potential of 200 mV of a) bare GC, b) PNSA/GC, c) PNMEAM/GC, and d) Au/PNMEAM/GC electrodes. A) In 1 M KCl at the scan rate of 100 $mV\,S^{-1}$ and B) Nyquist plots in 0.1 M KCl from 100 KHz to 100 mHz using an ac amplitude of 10 mV.

These results were also confirmed by analysis of the electrochemical impedance spectroscopy results. Electrochemical impedance spectroscopy can provide the information on the impedance changes of the electrode surface during the modification process, which is an effective method to probe the interfacial properties of surface-modified electrodes. As shown in Figure 3B, typical Nysquist plots ($-Z''$ vs Z') for 5 mM $[Fe(CN)_6]^{3-/4-}$ in 0.1 M KCl at the modified electrodes were obtained. In a Nyquist plot, the semicircle part in the high frequency corresponds to an interfacial charge-transfer mechanism and a straight line with a slope near unity in the low-frequency domains are the characteristic of semi-infinite diffusion phenomenon. The electron-transfer resistances (R_{et}) are equal to the semicircle diameters and they are 305, 672, 459, and 174 Ω for the bare GC, PNSA/GC, PNMEAM/GC, and Au/PNMEAM/GC electrodes, respectively. The highest R_{et} indicates that PNSA film electrografted onto the electrode surface creates a barrier to the interfacial-electron transfer. If the ester groups of PNSA reacted with amines of aminoethanethiol, the barrier of the electrode interface could decrease. After the Au NPs were linked on the electrode surface, although the thin film still lies between the Au NPs and electrode, the attached Au NPs serve as an electron relay station, this could greatly facilitate the electron tunneling through the film. Therefore, the electrode can be seen to perform better than the bare electrode. These results were consistent with the cyclic voltammetry results. The Au NPs covalently linked on the electrografting film are, therefore, ideal substrates to study the redox properties of enzymes owing to their rapid electron-transfer process.

Direct Electrochemistry of HRP Immobilized on an Au/PNMEAM/GC Electrode

To study the electrocatalytic behavior of an enzyme film on the electrode toward H_2O_2 and discern the contribution of Au NPs, an HRP/Au/PNMEAM/GC electrode was investigated. Figure 4A shows the CVs of HRP/Au/PNMEAM/GC electrode in the absence (a) and presence (b) of 300 μM H_2O_2. In the absence of H_2O_2, a couple of redox peaks corresponding to Fe^{III}/Fe^{II} of HRP were observed. Its anodic and cathodic peak potentials were located at −0.153 V and

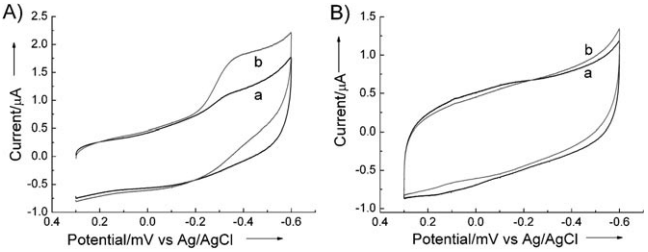

Figure 4. A) Cyclic voltammograms of HRP/Au/PNMEAM/GC and B) Au/PNMEAM/GC electrodes in the absence (curve a) and presence (curve b) of 300 μM H_2O_2 in the 0.02 mM PBS (pH 7.0) at the scan rate of 100 $mV\,S^{-1}$.

© 2010 Wiley-VCH Verlag GmbH & Co. KGaA, Weinheim

−0.328 V versus Ag/AgCl, corresponding to the oxidation and reduction of the electroactive centers of the immobilized HRP. This result suggests that Au NPs act as nanoscale electrical wires and facilitate the direct-electron transfer between the enzyme and the electrode surface. According to formula, $Q = nFA\Gamma^*$, in which A is the geometrical surface area of the electrode, n is the electron-transfer number, F is Faraday's constant, and Q is the integrating reduction peak-area of HRP. The surface concentration of the electroactive HRP (Γ^*) on the electrode surface can be estimated to be 6.4×10^{-12} mol cm^{-2}. Assuming one molecule with the long axis parallel to the electrode surface, the theoretical monolayer coverage of HRP was estimated to be 3.95×10^{-12} mol cm^{-2} on the basis of the crystallographic dimensional structure of HRP ($15.9\times15.9\times11.4$ nm)[35]. The obtained value of Γ^* was about 1.7 times more than the theoretical monolayer coverage. This implies that the Au/PNMEAM modified electrode surface is rough and provides more anchoring sites for the adsorption of HRP than the flat surface.

After the addition of 300 μM H_2O_2 to the PBS, the typical reduction peaks of H_2O_2 increased dramatically. With increasing the concentration of H_2O_2, the reduction peak current of HRP Fe^{III} increased, which was accompanied by the decrease of the oxidation current of HRP Fe^{II}. The reaction of hydrogen peroxide catalyzed by HRP may be described by the following mechanisms[37] in Equations (1) to (5):

$$\text{HRP } Fe^{III} + H_2O_2 \rightarrow \text{Compound I} + H_2O \quad (1)$$

$$\text{Compound I} + H_2O_2 \rightarrow \text{HRP } Fe^{III} + O_2 + H_2O \quad (2)$$

$$\text{HRP } Fe^{III} + H^+ + e^- \rightleftharpoons \text{HRP } Fe^{II} \text{ at electrode} \quad (3)$$

$$\text{HRP } Fe^{II} + O_2 \rightarrow \text{HRP } Fe^{II}-O_2 \text{ fast} \quad (4)$$

$$\text{HRP } Fe^{II}-O_2 + 2H^+ + 2e^- \rightarrow \text{HRP } Fe^{II} + H_2O_2 \text{ at electrode} \quad (5)$$

The chemical reaction increased the reduction current of HRP Fe^{III} to form the catalytic current. For comparison, as shown in Figure 4B, the reduction of H_2O_2 for Au/PNMEAM/GCE was observed. The reduction current was lower than that for HRP/Au/PNMEAM/GCE. These results showed that the immobilized HRP retained its electrocatalytic activity towards H_2O_2, and the Au NPs also enhanced the electrocatalytic reduction of H_2O_2.

Amperometric Response of HRP/Au/PNMEAM/GC Electrode Toward H_2O_2

Figure 5A shows the amperometric response of an HRP/Au/PNMEAM/GC electrode on successive addition of 50 μM H_2O_2 into 10 mL PBS (pH 7.0) at the applied potential of −0.3 V versus Ag/AgCl. The corresponding calibration curve is shown in Figure 5B. A subsequent addition of H_2O_2 to the stirring PBS led to a remarkable increase of the reduction current, and the time of achieving 95% of the steady-state current was within 5 s. From the calibration curve, it was estimated that the HRP/Au/PNMEAM/GC electrode could work linearly in H_2O_2 solution in a concentration range of 50–700 μM with a correlation coefficient of 0.997. The current saturated at high H_2O_2 concentration, exhibiting the characteristics of the Michaelis–Menten kinetics. Owing to the wide linear range, after the addition of 1.2 mM H_2O_2, the saturation of the response current at high concentration was not clear. This indicated that the HRP enzymes immobilized in the Au/PNMEAM composite film had high catalytic activities to H_2O_2. The sensitivity was estimated as 0.39 μA mM^{-1} cm^{-2} by calculating the slope of the linear range. The detection limit was 10 μM when the signal-to-noise ratio was 3.

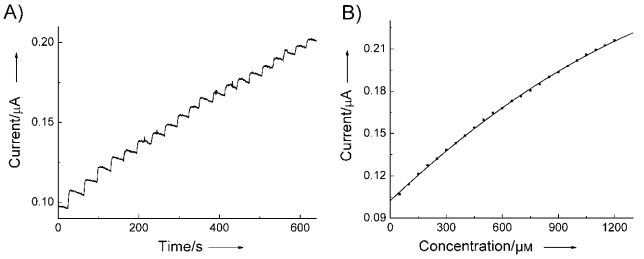

Figure 5. Amperometric response of A) HRP-modified GC electrode on successive addition of 50 μM H_2O_2 into 10 mL PBS (pH 7.0) at the applied potential of −0.3 V versus Ag/AgCl and B) the corresponding current-concentration calibration curve.

The apparent Michaelis–Menten constant (K_m^{app}), which indicates the enzyme-substrate kinetics for the biosensor, can be calculated from the Lineweaver–Burk equation, Equation (6)[38]:

$$\frac{1}{i_{ss}} = \frac{K_m^{app}}{i_{max}}\left(\frac{1}{C}\right) + \frac{1}{i_{max}} \quad (6)$$

in which i_{ss} is the steady-state current, C is the concentration of glucose, K_m^{app} is the apparent Michaelis–Menten constant and i_{max} is the maximum current. The apparent Michaelis–Menten constant K_m^{app} usually characterizes the biological activity of immobilized enzyme since it indicates the enzyme-substrate kinetics for the enzyme electrode. Also $K_m^{app} = (k_2+k_p)/k_1$, is the ratio of the rate at which the enzyme-substrate forms complex (ES) (k_1) to the rate at which ES dissociates (k_2+k_p). The dissociation of ES is the sum of the rate that the substrate dissociates from the enzyme before it undergoes the enzyme catalyzed reaction (k_2) and the dissociation rate of product following the reaction (k_p). The K_m^{app} also indicates the apparent affinity of the substrate for the enzyme. The enzyme with the lowest K_m^{app} value has the highest apparent affinity for the substrate. From the curve of i^{-1} versus C^{-1}, K_m^{app} was estimated to be 0.48 mM, which is smaller than the reported values of Au NPs/cystamine modified gold electrode,[33,34] The smaller K_m^{app} indicated that the HRP immobilized on the Au/PNMEAM modified electrode retained higher enzymatic activity for H_2O_2 reduction and implied that the present electrode exhibited better affinity

 © 2010 Wiley-VCH Verlag GmbH & Co. KGaA, Weinheim

to H_2O_2 than the reported sensors.

The stability of the HRP/Au/PNMEAM modified electrode was investigated by the measurement of the response to 100 μM H_2O_2 in the PBS at the applied potential of −0.3 V versus Ag/AgCl. The relative standard deviation (RSD) was about 2.7% for 10 successive assays. When not in use, the electrode was stored in PBS (pH 7.0) at 4°C. It retained 89% of its initial current response after three weeks. The long-term stability indicated that the strong Au/PNMEAM adhering film provided a biocompatible microenvironment for the immobilized enzymes to retain its bioactivity.

Conclusions

In summary, the electrografting of a thiol-terminated film to a glassy carbon electrode is a simple and versatile approach to strongly attach Au NPs. A mediator-free H_2O_2 biosensor was constructed based on HRP immobilized in a composite film of poly(*N*-mercaptoethyl acrylamide) and Au nanoparticles. The results revealed that HRP retained its biocatalytic activities and exhibited facilitated direct-electron transfer between the HRP and the underlying electrode. The HRP/Au/PNMEAM modified electrode showed a fast response and wide linear range toward reduction of hydrogen oxide and long-term stability. The Michaelis–Menten constant for the prepared electrode was smaller than the values produced by the previously researched Au NPs immobilized on a cystamine-modified gold electrode. Our results demonstrated that the combination of electrografting and Au NPs was a useful method to promote the electrochemical properties of HRP, and could be extended to the study of the direct electrochemistry of other redox enzymes and their sensing applications.

Experimental Section

Materials

Horseradish peroxidase (HRP, from *Aspergillus niger* (E.C. 1.1.3.4), 196000 units g^{-1}) was purchased from Beijing Dingguo Biotechnology Co. Ltd. *N*-succinimidyl acrylate (NSA) and tetrabutylammonium perchlorate (TBAP) were purchased from Sigma–Aldrich. All the analytic grade reagents were purchased from the Beijing Chemical Company and used without further purification. The water used was redistilled. The supporting electrolyte was 20 mM phosphate buffer solution (PBS) prepared with KH_2PO_4 and Na_2HPO_4. The buffer solution was purged with highly purified nitrogen for at least 30 min and the nitrogen atmosphere was kept during the electrochemical measurements.

Synthesis

Preparation of Au nanoparticles: Gold nanoparticles were prepared according to a conventional procedure.[39] 20 mL of 0.25 mM sodium citrate and 0.25 mM aqueous chloroauric acid were mixed uniformly. 600 μL of a freshly prepared aqueous solution of 0.1 mM $NaBH_4$ was then quickly added to the mixture for several minutes with vigorous stirring until the solution turned wine-red in color. After prepared for 2–5 h, the particles in this solution were used.

Preparation of HRP/Au/PNMEAM/glassy carbon electrode: Prior to the surface modification, the glassy carbon electrode (3 mm diameter) was polished with alumina powder, then rinsed thoroughly with redistilled water, and ultrasonically agitated successively in ethanol and redistilled water, each for 3 min. The procedures of the surface modification are depicted in Scheme 1. N-succinimidyl acrylate (NSA) was first electrografted by voltammetry in dimethylformamide with 0.05 M TEAP added as a conducting salt. Then the electrode was immersed in aminoethanethiol solution (1 mM) for 24 h to form poly(*N*-mercaptoethyl acrylamide) (PNMEAM) which provided thiol groups for the further immobilization of Au NPs. After reaction for 12 h, the Au/PNMEAM/GC electrode was kept in HRP solution for 12 h. Finally, the HRP/Au/PNMEAM/GC electrode was washed with buffer solution and preserved in a refrigerator at 4°C until use.

Instrumentation

Cyclic voltammetric and amperometric measurements were carried out by using a CHI 630B electrochemical workstation (CHI Inc., USA). Electrochemical Impedence experiments were performed by using PARSTAT 2273 (Princeton Applied Research, USA). A conventional three-electrode cell (10 mL) was used, which was composed of the modified glassy carbon electrode, as the working electrode, an Ag/AgCl (saturated KCl) electrode, as the reference electrode, and a platinum foil electrode, as the counter electrode. All potentials were measured and reported versus the Ag/AgCl (saturated KCl). The impedance measurements were performed in the presence of 5 mM $[Fe(CN)_6]^{3-/4-}$ in 0.1 M KCl from 100 KHz to 100 mHz at an ac amplitude of 10 mV under a bias potential of 200 mV conditions. ATR-FTIR spectra were obtained by using a PerkinElmer Spectrum GX spectrometer (PerkinElmer Company, USA). The surface morphology of the electrode was observed by using scanning electron microscopy (SEM, Hitachi 4200).

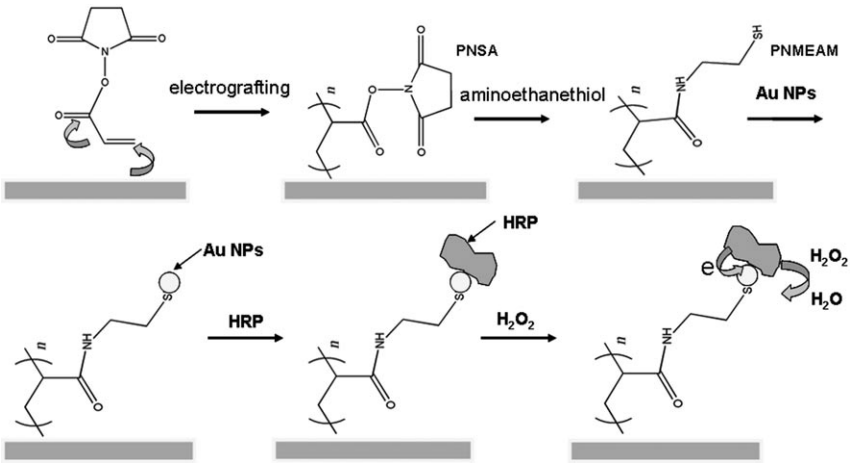

Scheme 1. Schematic illustration of the construction of HRP biosensor. The glassy carbon electrodes were initially electrografted with poly(*N*-succinimidyl acrylate) (PNSA) to produce strongly anchored coating, followed by reacting with aminoethanethiol to form poly(*N*-mercaptoethyl acrylamide) (PNMEAM), and then incubated in solutions of the negatively charged Au NPs and positively charged HRP. Finally, when certain amount of H_2O_2 was added, the electrons of reduced HRP Fe^{III} were transferred to the electrode surface through Au NPs.

© 2010 Wiley-VCH Verlag GmbH & Co. KGaA, Weinheim

Acknowledgements

This work was partly supported from the National Natural Science Foundation of China (No. 20975060) and National Basic Research Program of China (No. 2007CB310500).

[1] M. Mizoguchi, M. Ishiyama, M. Shiga, *Anal. Commun.* **1998**, *35*, 71–74.
[2] J. Kremeskotter, R. Wilson, D. J. Schiffrin, B. J. Luff, J. S. Willkinson, *Meas. Sci. Technol.* **1995**, *6*, 1325–1328.
[3] C. X. Cai, J. Chen, *Anal. Biochem.* **2004**, *332*, 75–83.
[4] Y. H. Li, F. Lu, Y. Tu, Z. F. Ren, *Nano Lett.* **2004**, *4*, 191–195.
[5] X. B. Lu, J. H. Zhou, W. Lu, Q. Liu, J. H. Li, *Biosens. Bioelectron.* **2008**, *23*, 1236–1243.
[6] G. Wang, N. M. Thai, S. T. Yau, *Electrochem. Commun.* **2006**, *8*, 987–992.
[7] W. Z. Jia, K. Wang, Z. J. Zhu, H. T. Song, X. H. Xia, *Langmuir* **2007**, *23*, 11896–11900.
[8] P. W. Barone, R. S. Parker, M. S. Strano, *Anal. Chem.* **2005**, *77*, 7556–7562.
[9] J. Anzai, H. Takeshita, Y. Kobayashi, T. Osa, T. Hoshi, *Anal. Chem.* **1998**, *70*, 811–817.
[10] Q. Zhang, L. Zhang, J. H. Li, *J. Phys. Chem. C* **2007**, *111*, 8655–8600.
[11] D. Zhang, K. Zhang, Y. L. Yao, X. H. Xia, H. Y. Chen, *Langmuir* **2004**, *20*, 7303–7307.
[12] D. Cochin, A. Laschewsky, *Macromol. Chem. Phys.* **1999**, *200*, 609–615.
[13] Y. J. Ma, W. F. Dong, M. A. Hempenius, H. Möhwald, J. Vancso, *Angew. Chem.* **2007**, *119*, 1732–1735; *Angew. Chem. Int. Ed.* **2007**, *46*, 1702–1705.
[14] S. Gabriel, A. S. Duwez, R. Jérôme, C. Jérôme, *Langmuir* **2007**, *23*, 159–161.
[15] C. Jérôme, S. Gabriel, S. Voccia, C. Detrembleur, M. Ignatova, R. Gouttebaron, R. Jérôme, *Chem. Commun.* **2003**, 2500–2501.
[16] S. Voccia, S. Gabriel, H. Serwas, R. Jérôme, C. Jérôme, *Prog. Org. Coat.* **2006**, *55*, 175–181.
[17] A. J. Downard, *Eletroanalysis* **2000**, *12*, 1085–1096.
[18] S. Griveau, D. Mercier, C. Vautrin-Ul, A. Chaussé, *Electrochem. Commun.* **2007**, *9*, 2768–2773.
[19] G. Lécayon, Y. Bouizem, C. Le Gressus, C. Reynaud, C. Boiziau, C. Juret, *Chem. Phys. Lett.* **1982**, *91*, 506–510.
[20] S. Ameur, C. Bureau, J. Charlier, S. Palacin, *J. Phys. Chem. B* **2004**, *108*, 13042–13046.
[21] J. C. Harper, R. Polsky, D. R. Wheeler, S. M. Brozik, *Langmuir* **2008**, *24*, 2206–2211.
[22] S. Herrwerth, T. Rosendahl, C. Feng, J. Fick, W. Eck, M. Himmelhaus, R. Dahint, M. Grunze, *Langmuir* **2003**, *19*, 1880–1887.
[23] C. Jérôme, R. Jérôme, *Angew. Chem.* **1998**, *110*, 2639–2642; *Angew. Chem. Int. Ed.* **1998**, *37*, 2488–2490.
[24] X. L. Luo, A. J. Killard, A. Morrin, M. R. Smyth, *Anal. Chim. Acta* **2006**, *575*, 39–44.
[25] T. Xu, N. Zhang, H. L. Nichols, D. L. Shi, X. J. Wen, *Mater. Sci. Eng. C* **2007**, *27*, 579–594.
[26] J. M. Xu, W. Li, Q. F. Yin, Y. L. Zhu, *Electrochim. Acta* **2007**, *52*, 3601–3606.
[27] Q. Liu, X. B. Lu, J. Li, X. Yao, J. H. Li, *Biosens. Bioelectron.* **2007**, *22*, 3203–3209.
[28] H. Y. Gu, A. M. Yu, H. Y. Chen, *J. Electroanal. Chem.* **2001**, *516*, 119–126.
[29] S. Yang, W. Z. Jia, Q. Y. Qian, Y. G. Zhou, X. H. Xia, *Anal. Chem.* **2009**, *81*, 3478–3484.
[30] X. J. Han, W. L. Cheng, Z. L. Zhang, S. J. Dong, E. K. Wang, *Biochim. Biophys. Acta Bioenerg.* **2002**, *1556*, 273–277.
[31] X. Jiang, L. Zhang, J. G. Jiang, X. H. Qu, E. K. Wang, S. J. Dong, *ChemPhysChem* **2005**, *6*, 1613–1621.
[32] Y. Liu, H. Y. Liu, N. F. Hu, *Biophys. Chem.* **2005**, *117*, 27–37.
[33] S. Bharathi, M. Nogami, S. Ikeda, *Langmuir* **2001**, *17*, 1–4.
[34] C. H. Wang, C. Yang, Y. Y. Song, W. Gao, X. H. Xia, *Adv. Funct. Mater.* **2005**, *15*, 1267–1275.
[35] Y. Xian, Y. Hu, F. Liu, Y. Xian, H. Wang, L. Jin, *Biosens. Bioelectron.* **2006**, *21*, 1996–2000.
[36] Z. M. Liu, Y. Yang, H. Wang, Y. L. Liu, G. L. Shen, R. Q. Yu, *Sens. Actuators B* **2005**, *106*, 394–400.
[37] Y. Xiao, H. X. Ju, H. Y. Chen, *Anal. Biochem.* **2000**, *278*, 22–28.
[38] S. F. Wang, T. Chen, Z. L. Zhang, D. W. Pang, *Electrochem. Commun.* **2007**, *9*, 1337–1342.
[39] H. L. Guo, D. Y. Liu, X. D. Yu, X. H. Xia, *Sens. Actuators B* **2009**, *139*, 598–603.
[40] A. C. Onuoha, X. Zu, J. F. Rusling, *J. Am. Chem. Soc.* **1997**, *119*, 3979–3986.
[41] R. A. Kamin, G. S. Wilson, *Anal. Chem.* **1980**, *52*, 1198–1205.
[42] N. R. Jana, L. Gearheart, C. J. Murphy, *J. Phys. Chem. B* **2001**, *105*, 4065–4067.

Received: September 24, 2009
Published online: February 9, 2010

 © 2010 Wiley-VCH Verlag GmbH & Co. KGaA, Weinheim